Chapter 50
Structural Study of Perovskite Materials for SOFCs Applications

O. Koleva, S. Simeonov, S. Kozhukharov, and M. Machkova

Abstract Solid oxide fuel cells (SOFCs) are a forward-looking approach for highly efficient, environmentally friendly power generation. Economically competitive SOFC systems appear suited for commercialization, but widespread market penetration requires continuous innovation of materials and fabrication processes to enhance system lifetime and reduce costs. A very effective way for enhancing the cell efficiency is to the improve properties of the cathode by achieving conductivity through oxygen ions while at the same time the material maintains the electronic one. As it is known, revealing the microstructure of a material opens the door for improving its macroscopic properties and consequently its practical use. The perovskite family, including Ruddlesden-Popper phases, successfully fulfills many of the requirements for SOFC cathode materials application. Therefore, in the present work two different perovskite compositions, i.e., $La_{1.7}Sr_{0.3}CuO_4$, and $Nd_{1.6}Sr_{0.4}NiO_4$ have been object of structural studies by X-ray diffraction and IR spectroscopy. An adequate conclusion for each of the spectra is presented.

Keywords SOFC • Cathodes • Perovskite-type materials • IR spectroscopy • Structural study

50.1 Introduction

Solid oxide fuel cells (SOFCs) are a forward-looking approach for highly efficient, environmentally friendly power generation. A SOFC is a high-temperature (800–900 °C) device that converts the chemical energy of fuels (such as hydrogen,

O. Koleva (✉)
Department of Silicate Technology, Laboratory for Advanced Materials Research, University of Chemical Technology and Metallurgy – Sofia, 8 "Kl. Ohridski" Blvd., 1756 Sofia, Bulgaria

Section of Solid State Electrolytes, Institute of Electrochemistry and Energy Systems (IEES), Bulgarian Academy of Sciences, Bl.10 Acad. G. Bonchev Str., 1113 Sofia, Bulgaria
e-mail: ofeliya.kostadinova@gmail.com

S. Simeonov • S. Kozhukharov • M. Machkova
Department of Silicate Technology, Laboratory for Advanced Materials Research, University of Chemical Technology and Metallurgy – Sofia, 8 "Kl. Ohridski" Blvd., 1756 Sofia, Bulgaria

P. Petkov et al. (eds.), *Nanoscience Advances in CBRN Agents Detection, Information and Energy Security*, NATO Science for Peace and Security Series A: Chemistry and Biology, DOI 10.1007/978-94-017-9697-2_50

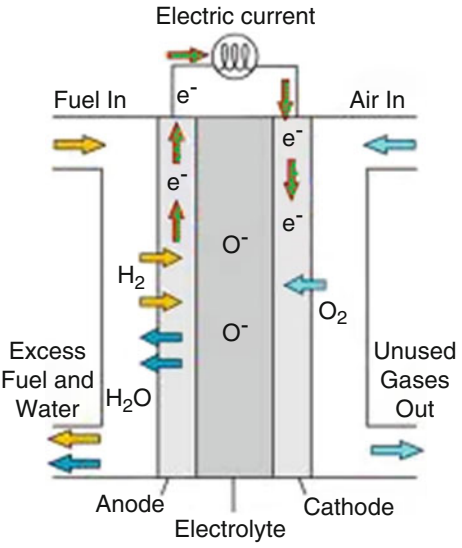

Fig 50.1 Basic scheme of a SOFC

natural gas or other hydrocarbons) directly into electricity through electrochemical oxidation of the fuel with an oxidant, typically oxygen from air. Figure 50.1 shows the basic scheme and work principle of a SOFC. The conversion of chemical into electrical energy is achieved by separating the chemical reaction into two electrochemical reactions (50.1 and 50.2) taking place inside the porous electrodes. At the negative electrode (anode) the hydrogen and carbon monooxide are oxidized with oxygen ions from the electrolyte to form water and carbon dioxide, respectively. The resulting electrons are transported through an external circuit to the positive electrode (cathode) where they are used to reduce oxygen to oxygen ions which are subsequently transported through the electrolyte to the negative electrode.

$$\text{Cathode reaction} : \tfrac{1}{2}\,O_2 - 2e^- \rightarrow O^{2-} \tag{50.1}$$

$$\text{Anode reaction} : H_2 + O^{2-} \rightarrow H_2O + 2e^- \tag{50.2}$$

Economically competitive SOFC systems appear poised for commercialization, but widespread market penetration requires continuous innovation of materials and fabrication processes to enhance system lifetime and reduce cost [1].

An effective approach to cost reduction is the lowering of the operating temperature without inferring performance losses [1]. This can be achieved either by using of thin electrolytes or electrolytes with high ionic conduction (Ce-based doped electrolyte) [2–4]. In these cases it is necessary to develop cathode materials which are adapted to the low-temperature electrolyte and which, at the same time, possess a high conductivity and low cathodic polarization at intermediate temperatures to diminish energy losses from the ohmic resistivity [5]. It was found that decreasing the electrolytic membrane width leads to a decrease in

electrolytic resistivity. This had been attained in SOFCs with planar geometry by using an additional porous anode, on which firstly an uniform thin film (10 μm) from the electrolyte material and thereafter a porous cathode material with a thickness around 50 μm are deposited. For such a type of configuration a very high energy density at temperatures from 700 to 800 °C were achieved.

On the other hand, a very effective way to improve the cell efficiency is to change the properties of the cathode by achieving oxygen ion conductivity while at the same time the material maintains the electronic one. In such a way the process is influenced into two directions: it is shifted outside to triple-phase boundaries (TPB) and it is performed on the surface. A TPB is a point where air, electrolyte and cathode electrode meet each other. It is believed that the cathode properties can be improved by increasing the number of triple phase boundaries.

From a general viewpoint, mixed electronic and ionic conducting oxides (MEIC) can be formulated as $(A, A')_n(M, M')_mO_{x \pm \delta}$, where A and A′ are either rare-earth or alkaline earth cations of large size and M and M′ are 3d elements, respectively. Depending on the n/m ratio, various structural types can be formed, for instance perovskite or derived compounds of the Ruddlesden-Popper type ($A_2MO_{4+\delta}$, where A = La, Nd, Pr, Sr, and M = Ni, Cu, Co). Varying the nature of the A and A′ cations and the A/A′ ratio, as well as the nature of M and M′, results, firstly, in mixed valences of the M, M′ cations, which confers usually a p-type electronic conductivity, and secondly either to a sub- or an over-stoichiometry of oxygen, which can induce ionic conductivity. The perovskite family which form the so-called Ruddlesden-Popper phases successfully fulfill above mentioned requirements for SOFCs cathode materials [6]. The main feature of most members of this family is that they exhibit some oxygen over stoichiometry associated with the mixed valence of the transition metal M-cations. Their structure (K_2NiF_4-type) is made up of sheets of (MO_6) elongated corner-sharing octahedra, interleaved by A_2O_2 layers with a NaCl-type structure in which additional oxygen atoms O_i can be inserted (Fig. 50.2). The amount of inserted oxygen atoms (δ) may reach values

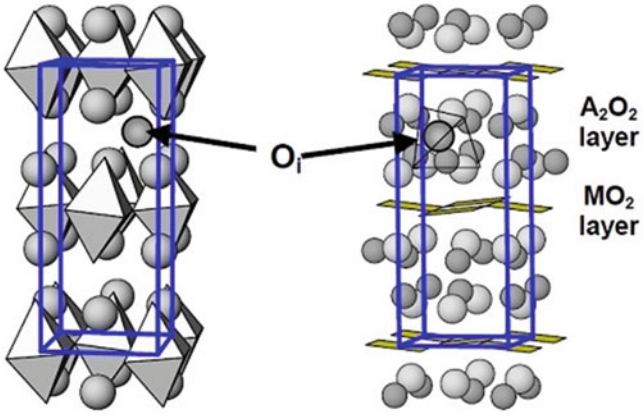

Fig. 50.2 Structure of $A_2MO_{4+\delta}$ compounds showing the location of interstitial oxygen atoms [6]

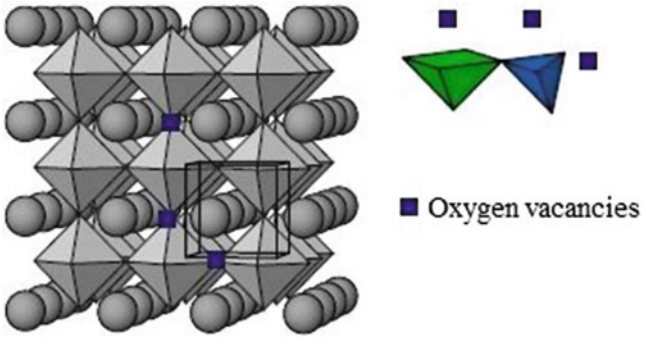

Fig. 50.3 Structure of $AMO_{3-\delta}$ perovskite showing the location of the oxygen vacancies [6]

as high as 0.22 for $Nd_2NiO_{4+\delta}$ or even 0.25 for electrochemically oxidized $La_2NiO_{4+\delta}$ [6]. They are located in tetrahedral sites $(O_IA)_4$, as shown in Fig. 50.3. Compared to the perovskite compounds, the oxygen transport in these materials is supposed to be quite different with respect to the non-stoichiometric type that involves interstitial oxygen atoms instead of oxygen vacancies. Basic properties of these materials have been studied [7, 8] using the $^{18}O/^{16}O$ isotope exchange/depth profile (IEDP) method. It has been proven that this family of compounds exhibit indeed larger oxygen bulk diffusion (D^*) and surface exchange (k) coefficients in comparison to the classical perovskite compounds.

Nevertheless, they exhibit some shortcomings which should be pointed out. The first one is the fact that they react with the zirconium-based electrolyte and form unwanted isolating phases. The others are related to the high costs of lanthanum oxide and the fact that the oxygen conductivity is limited to less than 10 % of the whole conductivity.

Taking into account the above discussion it becomes clear that it is necessary to develop new materials and compositions which could overcome these [9]. Therefore, in this study we synthesized and characterized structurally new compositions of advanced perovskite-like materials which are directly used as SOFC cathodes. For structural investigation we employed IR spectroscopy, a technique which is very powerful and can provide important information on the distinct structural units that built a material. As it is known, revealing the microstructure opens the door for improving the macroscopic properties and consequently the practical use of a material.

50.2 Experimental

In the present work the investigated compositions are $La_{1.7}Sr_{0.3}CuO_4$ and $Nd_{1.6}Sr_{0.4}NiO_4$, respectively. The samples origin is CerPoTech AS Company, Norway. The synthesis followed a standard solid state reaction procedure,

i.e. thermal treating process at 1,250 °C. In order to reveal the existing phases in the samples, we performed XRD analysis by a Bruker D8-Advance using Cu K_α radiation in the 2θ range from 10 to 80°. The measurement took place at ambient temperature with 0.020° steps and a step time of 17.5 s. IR spectra were measured with a FT-IR spectrometer model VARIAN 660-IR FT-IR. Test samples were prepared in KBr tablets and measured at ambient temperature in the spectral range between 4,000 and 400 cm^{-1}.

50.3 Results and Discussion

Although the method is very useful, the IR spectroscopy bears some limitations. For instance, one of the reasons for the difficulties in studying the IR-active phonons is the large in-plane polarizability due to the presence of free carriers. This causes masking of the phonon-related structure and allows only the c-axis vibrations to be observed [10, 11]. For this reason, most of IR-active phonon studies of similar systems were focused on the frequency region from 50 to 520 cm^{-1} [12–15]. Few publications have been found about IR study in the frequency region between 600 and 700 cm^{-1} [11, 16, 17].

50.3.1 Structural Behavior of $La_{1.7}Sr_{0.3}CuO_4$ System

50.3.1.1 X-ray Diffraction Investigation

X-ray diffraction analysis of the $La_{1.7}Sr_{0.3}CuO_4$ system, presented in Fig. 50.4 displays diffraction maxima for only one compound, i.e. $La_{1.7}Sr_{0.3}CuO_4$. This result suggests that the sample is well-synthesized and homogenous.

50.3.1.2 Infrared Study

The IR spectrum of $La_{1.7}Sr_{0.3}CuO_4$ composition is presented in Fig. 50.5. At lower frequencies the spectrum contains two modes located at 503 and 668 cm^{-1}, respectively. Due to above mentioned limitations of the method, their assignment is not straightforward. While studying a sample from the same system but with different compositions, i.e. $La_{2-x}Sr_xCuO_4$, $0 \leq x \leq 0.125$ %, Napoletano et al. [16] discussed the two most pronounced peaks in their spectra, located at 684 cm^{-1} and 514 cm^{-1}, respectively. Taking into account the stability of the peak intensity, the authors attributed the latter band in the undoped La_2CuO_4 to the La–O asymmetric stretching mode. This assignment is also supported by its slight shift to lower frequencies with increasing Sr concentration. Actually, Sr doping causes the apical

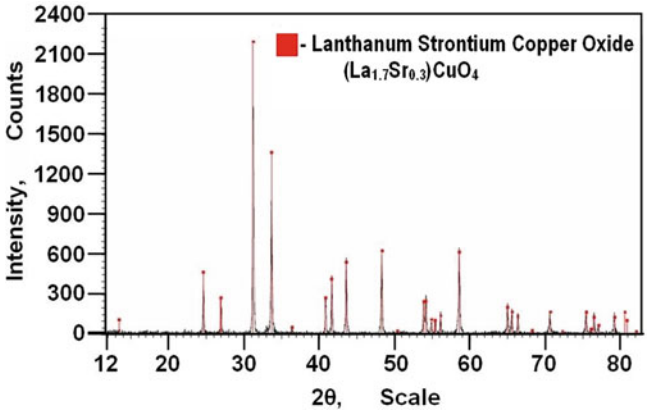

Fig. 50.4 XRD diffraction pattern of a $La_{1.7}Sr_{0.3}CuO_4$ compound

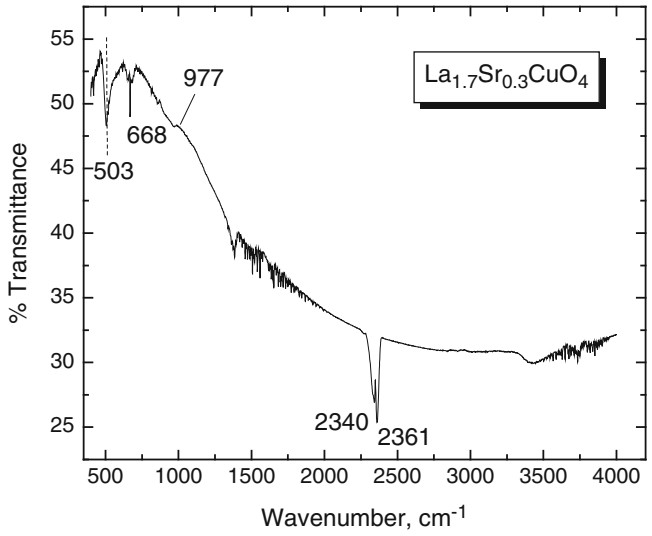

Fig. 50.5 The infrared spectrum of a $La_{1.7}Sr_{0.3}CuO_4$ sample

La(Sr)-O bond length to increase significantly resulting in a gradual shift down of the corresponding stretching modes.

Having in mind that all these findings are valid for a maximum Sr content $x = 0.125$ %, it seems quite logical to assume that an increase of the Sr concentration to $x = 0.3$ % as in our case would lead to larger down-shift, reaching

eventually 503 cm^{-1}. Therefore, taking into account both, the different Sr concentrations and the band shifting in comparison to the one found in the work of Napoletano et al. [18], we attributed the mode located at 503 cm^{-1} in our spectrum as a contribution from La–O asymmetric stretching vibrations. Assignments of the next higher frequency band found at 668 cm^{-1} are contradictory. As it was already mentioned, in the work of Napoletano et al. [16] the authors discuss a peak located at 684 cm^{-1}. In order to interpret it, they followed the idea that the random substitution of La ions by alkali earth ions results in increased apical O–Cu bond lengths and slightly decreased in-plane O–Cu bond lengths.

As it is known, the higher frequency bands should certainly be assigned to vibrational modes primarily involving the stretching of shorter and stronger bonds. In the present case such bonds are the basal Cu–O ones with a length of 1.90 Å and perhaps La–O bonds with a length of 2.35 Å. Stretching modes of the longer apical Cu–O bonds (length 2.5 Å) are expected at lower frequencies. Following this concept, as a conclusion, the authors suppose that the band situated at 684 cm^{-1} is due to the superposition of two asymmetric stretching modes of CuO_4 "squares". They ascribe the steady reduction of this peak by doping from $0 \leq x \leq 0.125$ %, to the increased symmetry of the unit cell when the latter changes from orthorhombic to tetragonal. This alteration results in losing the splitting of the asymmetric Cu–O stretching effect. A similar phenomenon has been observed also in other works [11, 17]. In the work of Pu et al. [11], where the authors studied $La_{1.85+x}Sr_{0.15-x}Cu_{1-x}Li_xO_y$, they observed the disappearance of the 683 cm^{-1} absorption band. Although that they observed the same effect as in the work of Napoletano et al. [16], they give a different explanation. They proposed [11] the idea that the free carriers can cause IR active phonon in-plane polarization and mask phonon-related structures in the spectra. These so-called screening effects have also been reported in other works [15, 18]. Thus, the authors ascribe the disappearance of the IR vibrational mode at 696 cm^{-1} in their spectra to screening effects of charge carriers. With Li content increasing further, Li doping at Cu sites replaces Cu^{2+} spins and destroys the Cu^{2+} spin correlation. This effect inspires the charge carriers to change from a delocalized state to a localized state. Then this frequency peak appears again but at a higher frequency of ~705 cm^{-1} when the dopant concentration exceeds $x \geq 0.2$. The authors attributed the newly appearance of the band to the monotonous decrease of the lattice parameter *a* which is in good agreement with the gradual hardening of the Cu–O(1) stretching modes in the $La_2Cu_{1-x}Li_xO_y$ system. Thus, the IR mode at 683 cm^{-1} shifts to 703 cm^{-1}.

It is known that the Cu–O stretching modes are closely related to the Cu–O bond length. The shift of the IR modes can be interpreted based on the changes of the lattice parameters *a* and *c* [11]. Hence, an increase of the distance between planar O and Cu^{2+} will result in downward shifting of the Cu–O(1) stretching modes to lower frequencies [17]. We suppose that disappearance of the 684 cm^{-1} band in the work of Napoletano et al. [18] might be due to the screening effect that was described by other authors [11, 15, 18]. Since the Sr content in their study does not exceeds 0.125 %, the band does not appear again. In our study, adding a quantity of more than 0.125 % [19] stimulates two effects. The first one is related

to the appearance of a mode, which is due to planar Cu-O again. The second effect concerns the shifting of the same mode to lower frequencies. The latter has been caused by an increase of the planar O and Cu^{2+} distance.

Turning our attention to higher frequencies, we observe a band located at 977 cm^{-1}. This mode most probably is due to vibrations of water molecules. In the spectral range between 2,340 and 2,365 cm^{-1} two vibrational modes appear. They are related to vibrations of CO_2 molecules. In the very high frequency region, a slight peak appears at 3,415 cm^{-1}. Most probably, this peak is a contribution of O-H stretching vibration of H_2O molecules [20]. Both, water molecules and CO_2, are contribution from absorption effect from the air.

50.3.2 Structural Behavior of $Nd_{1.6}Sr_{0.4}NiO_4$ System

50.3.2.1 X-ray Diffraction Investigation

A X-ray diffraction analysis of the $La_{1.7}Sr_{0.3}CuO_4$ system is shown in Fig. 50.6. The diffractograms displays diffraction maxima for two compounds, i.e. $Nd_{1.6}Sr_{0.4}NiO_4$ and small amount of Al. Aluminum appears as an impurity. Nevertheless, the sample is crystalline, without any detectable vitreous phase and homogeneous.

50.3.2.2 Infrared Study

Since this compound is innovative, only few publications have been found during our detailed searching. An IR spectrum of the investigated composition $Nd_{1.6}Sr_{0.4}NiO_4$ is presented in Fig. 50.7. Two indicative bands situated at 510 and 710 cm^{-1} are

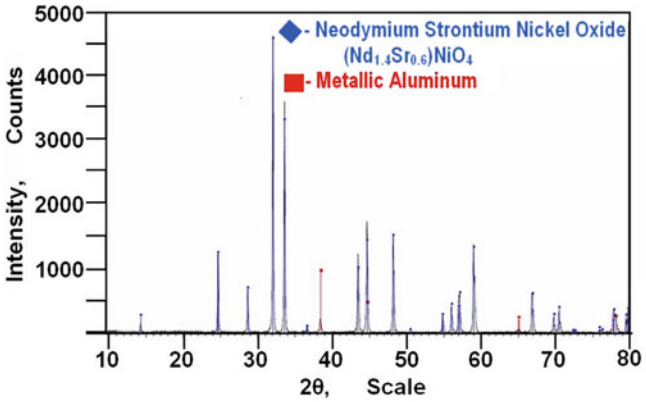

Fig. 50.6 XRD analysis of the $Nd_{1.6}Sr_{0.4}NiO_4$ system

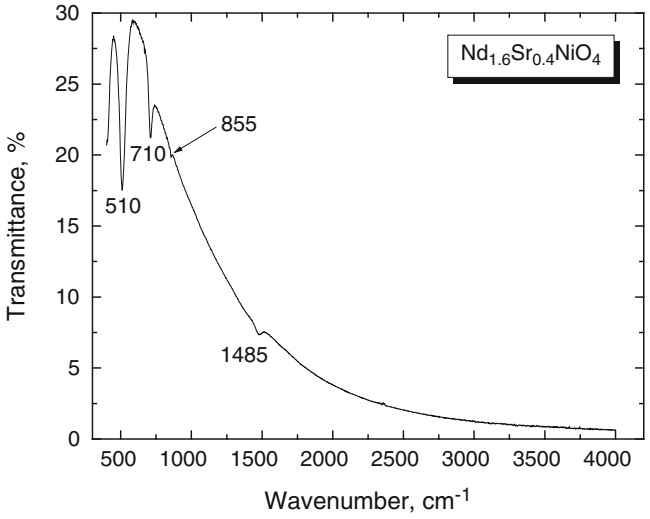

Fig. 50.7 The infrared spectrum of a $Nd_{1.6}Sr_{0.4}NiO_4$ powder sample

examined. According to Ref. [21], these two modes are characteristic for Ni-O stretching vibrations.

In addition, two more weak bands positioned at 855 and 1,485 cm $^{-1}$ are observed. According to Zhu et al. [22] both peaks are contributions from $SrCO_3$ vibrations. More exactly, they originate from both inorganic carbonate C-O stretch at 1,510–1,410 cm^{-1} and C-O out-of-plane bending in the wavenumber range from 880 to 860 cm^{-1}. Following the discussion carried out above, these small absorption bands may be due to CO_2 molecule vibrations. These structural units are typical for inorganic carbonates and are probably formed after the synthesis of the material due to CO_2 absorption from the air. No contributions from H_2O molecules, i.e. O-H stretching vibrations were registered.

50.4 Conclusions

Two different perovskite-type compositions, i. e. $La_{1.7}Sr_{0.3}CuO_4$ and $Nd_{1.6}Sr_{0.4}NiO_4$ were structurally investigated by X-ray diffraction and IR spectroscopy. On the base of X-ray diffraction analysis both samples seem well-synthesized and homogenous which is the first preliminary condition for the next studies and usage. Interpretation of the lanthanum-cuprate IR spectrum is not straightforward which has a two-fold origin: (i) higher La-content and appearance of the so-called screening effect which is typical for this system. Nevertheless, two characteristic bands were detected for this system and were attributed to La-O asymmetric stretching vibrations and to asymmetric Cu-O vibrations in CuO_4 squares,

respectively. The interpretation of IR spectrum of $Nd_{1.6}Sr_{0.4}NiO_4$ powder sample is simpler. Few vibrational modes were observed. Among them, two were found indicative and attributed to Ni-O stretching vibrations. Moreover, inorganic carbonate C-O vibrations from $SrCO_3$ were also observed. In brief, judging from this preliminary structural investigation, $La_{1.7}Sr_{0.3}CuO_4$ and $Nd_{1.6}Sr_{0.4}NiO_4$ are appropriate for cathode materials in SOFCs, which is in agreement with our preliminary results [23].

Acknowledgments The authors kindly acknowledge the financial support from the Bulgarian National Science Fund – project No. TK-X-1711

References

1. Barbucci A, Piccardo P, Carpanese MP, Viviani M (2006) In: Stoynov Z, Vladikova D (eds) Portable and emergency energy sources. Prof. Marin Drinov Publishing House, Sofia, p 329
2. Steele BCH (2000) Solid State Ionics 134:3
3. Will J, Mitterdorfer A, Kleinlogel C, Perednis D, Gauckler LJ (2000) Solid State Ionics 131:79
4. Mogensen M, Sammes NM, Tompsett GA (2000) Solid State Ionics 129:63
5. Fuel Cell Today (2007) Technology article solid oxide fuel cells. http://www.fuelcelltoday.com/media/pdf/surveys/2007-SOFC-Survey.pdf
6. Grenier JC, Bassat JM, Lalanne C, Mauvy F (2009) In: Vladikova D, Stoynov Z (eds) Proceedings international workshop "Advances and Innovations in SOFCs", Katarino, Bulgaria, 13–16 September 2009, p 21
7. De Souza RA, Kilner JA, Walker JF (2000) Mater Lett 43:43
8. Boehm E, Bassat JM, Steil MC, Dordor P, Mauvy F, Grenier JC (2003) Solid State Sci 5:973
9. Patent No US 20070207373: Solid oxide fuel cell cathode material (2007)
10. Genzel L, Wittlin A, Bauer M, Cardona M, Schronherr E, Simon A (1989) Phys Rev B 40:2170
11. Pu Q, Xu G, Zhang Z, Ding Z (2002) Physica C 370:269
12. Henn R, Kircher J, Cardona M (1996) Physica C 269:99
13. Henn R, Wittlin A, Cardona M, Uchida S (1997) Phys Rev B 56:6295
14. Humliček J, Litvinchuk AP, Kress W, Lederle B, Thomsen C, Cardona M, Habermeier HU, Trofimov IE, König W (1993) Physica C 206:345
15. Schutzmann J, Tajima S, Miyamoto S, Sato Y, Hauff R (1995) Phys Rev B 52:13665
16. Napoletano M, Amores JMG, Magnone E, Busca G, Ferretti M (1999) Physica C 319:229
17. Xu G, Pu Q, Zhang Z, Ding Z (2002) Physica C 370:101
18. Heyen ET, Kliche G, Kress W, König W, Cardona M, Rampf E, Prade J, Schröder U, Kulkarni AD, de Wette FW, Pinol S, Paul DM, Moran E, Alario-Franco MA (1990) Solid State Commun 74:1299
19. Wang SH, Song Q, Clayman BP (1990) Phys Rev Lett 64:1067
20. Kadinov G, Institute of Catalysis, Bulgarian Academy of Sciences, Laboratory of New catalytic and Nano-sized Catalysts, Private communications
21. Si-Wen L, Yu-Fang R (1995) Mater Res Bull 30:1505
22. Zhu J, Dehai X, Jing L, Xiangguang Y, Yue W (2005) J Mol Catal A Chem 234:99
23. Kozhukharov S, Machkova M, Kozhukharov V, Simeonov S (2013) Bulg Chem Commun 45(2):207